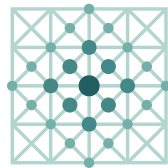


Mathematical modeling for all-solid-state batteries: Strain energy and Griffith criterion

Tuan Vo^{1,2}

Supervisors: Stefanie Braun¹, Claas Hüter², Manuel Torrilhon¹

(1) · RWTH Aachen University · Applied and Computational Mathematics · ACoM
(2) · Joint with Forschungszentrum Jülich · Institute of Energy and Climate Research · IEK-2



Applied and
Computational
Mathematics

RWTHAACHEN
UNIVERSITY

 **JÜLICH**
Forschungszentrum

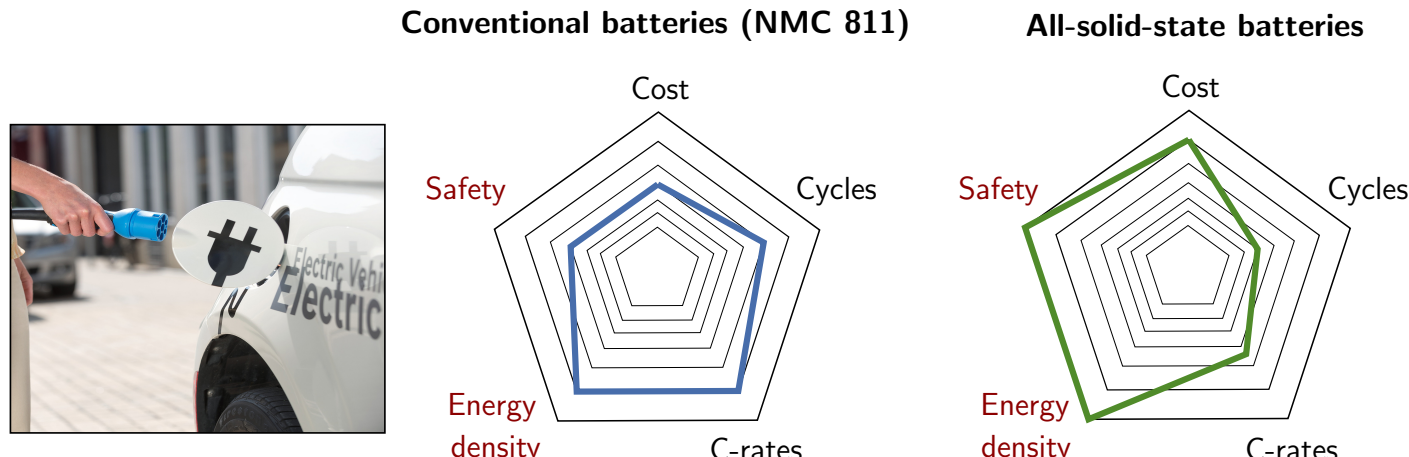
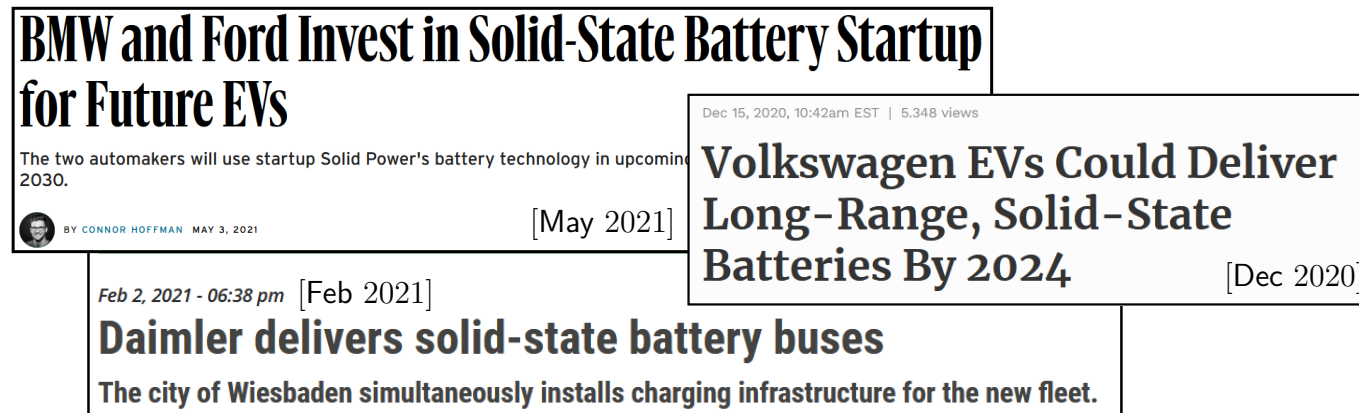
NUMAP-FOAM Summer School 2022 · September 22 · Cambridge, England

Contents

1. Motivation and overview
2. Mathematical modeling for thermodynamic-consistent solid-state electrolyte
3. Numerical implementation, representative results and applications
4. Summary and conclusions

1. Motivation and overview

All-solid-state battery means material made of anode, cathode and electrolyte are all of solid.



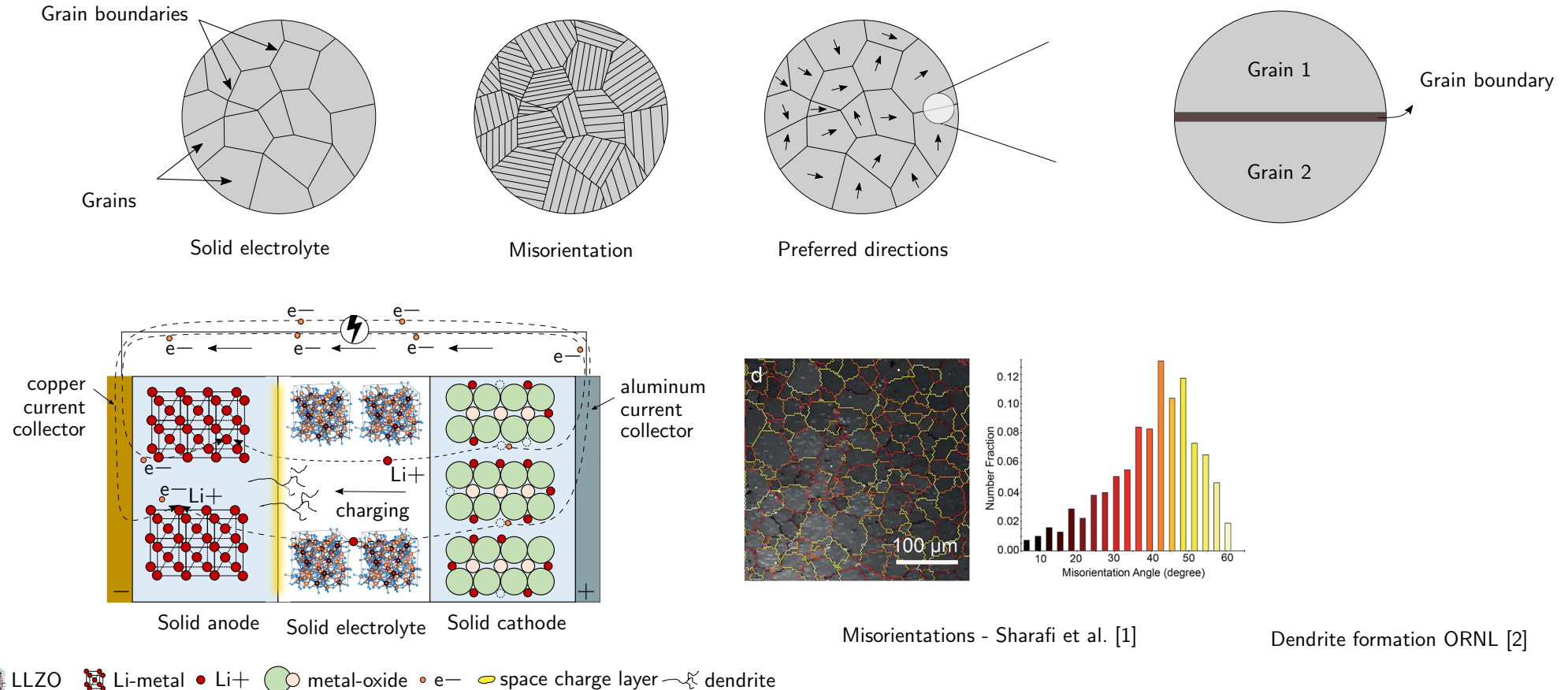
All-solid-state battery (ASSB) is outstanding compared to conventional Li-based battery due to

- *safety* (flammability & leakage)
- *high energy density*

→ Still, ASSBs exhibit natural issues of **ceramic-like** materials, which shall be taken into consideration (*safety*).

1. Motivation and overview

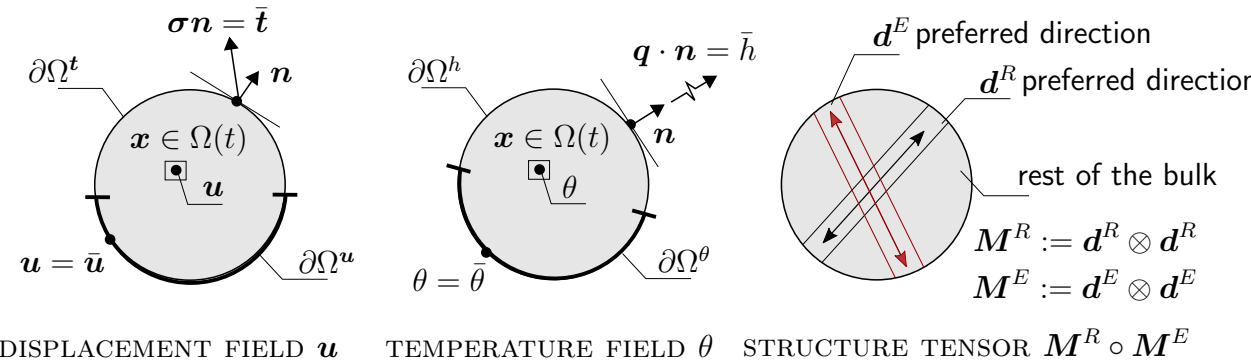
Grain boundaries and misorientation between grains govern direction of dendrites and fractures.



- Goals**
- A mathematical model holds **thermodynamical consistency**.
 - **Griffith criterion** and its correlation with **strain energy** and **surface energy**.
 - Representative results of **Griffith criterion**.

2. Mathematical modeling for thermodynamic-consistent solid-state electrolyte

Primary fields



- **Primary field variables and their gradients**

Displacement field and temperature field

$$\mathbf{u} : \begin{cases} \Omega \times \mathbb{R}_+ \rightarrow \mathbb{R}^3, \\ (\mathbf{x}, t) \mapsto \mathbf{u}(\mathbf{x}, t), \end{cases} \quad \text{and} \quad \theta : \begin{cases} \Omega \times \mathbb{R}_+ \rightarrow \mathbb{R}, \\ (\mathbf{x}, t) \mapsto \theta(\mathbf{x}, t), \end{cases}$$

Local action requires gradient of displacement field \mathbf{u} and temperature field θ

$$\boldsymbol{\varepsilon} = \nabla_s \mathbf{u}(\mathbf{x}, t), \quad \mathbf{g} := \nabla \theta(\mathbf{x}, t).$$

- **Kinematic relation:** Infinitesimal strain $\boldsymbol{\varepsilon}$

$$\boxed{\boldsymbol{\varepsilon} = \frac{1}{2} \left(\frac{\partial \mathbf{u}}{\partial \xi} + \left(\frac{\partial \mathbf{u}}{\partial \xi} \right)^\top \right)}$$

→ This kinematic relation is used for the current model of solid-state electrolyte.

2. Mathematical modeling for thermodynamic-consistent solid-state electrolyte

- **Summary of conservation laws:**

$$\frac{d}{dt} \int_{\Omega} (\cdot) d\Omega = \int_{\Omega} (\cdot)^{\text{action}} d\Omega + \int_{\partial\Omega} (\cdot)^{\text{action}} d\partial\Omega + \int_{\Omega} (\cdot)^{\text{production/source/sink}} d\Omega$$

Balance of mass

$$\dot{\rho} + \rho \operatorname{div} \mathbf{v} = 0$$

Balance of linear momentum

$$\rho \dot{\mathbf{v}} = \operatorname{div} \boldsymbol{\sigma} + \rho \mathbf{b}$$

Balance of energy

$$\rho \dot{e} = \boldsymbol{\sigma} : \dot{\boldsymbol{\epsilon}} + \rho r - \operatorname{div} \mathbf{q}$$

Balance of angular momentum $\boldsymbol{\sigma}^T = \boldsymbol{\sigma}$

where

$\rho(\mathbf{x}, t)$ is mass density per unit volume (puv); $\mathbf{b}(\mathbf{x}, t)$ body force puv; $\mathbf{v}(\mathbf{x}, t)$ velocity; $e(\mathbf{x}, t)$ internal energy puv; $\mathbf{q}(\mathbf{x}, t)$ heat flux; $r(\mathbf{x}, t)$ heat source puv; $\boldsymbol{\sigma}$ Cauchy stress and $\boldsymbol{\epsilon}$ infinitesimal strain.

Closure

#eqns	#unkns
1 _(mass)	+1(ρ)
3 _(Imom.)	+3(\mathbf{v})
1 _(energy)	+9($\boldsymbol{\sigma}$)
	+0(\mathbf{b})
	+0(r)
	+3(\mathbf{q})
	-3($\boldsymbol{\sigma}$)
	+1(η)
	+1(θ)
	+6($\boldsymbol{\sigma}$)
	+1(η)
	+3(\mathbf{q})
15	15

2. Mathematical modeling for thermodynamic-consistent solid-state electrolyte

- **Entropy inequality:** $\frac{d}{dt}(\text{Entropy}) - \text{Entropy power} \stackrel{!}{\geq} 0$

$$\text{Entropy Clausius-Planck inequality (CPI): } \boldsymbol{\sigma} : \dot{\boldsymbol{\varepsilon}} - \rho\eta\dot{\theta} - \rho\dot{\Psi} - \frac{1}{\theta}\mathbf{q} \cdot \nabla\theta \geq 0$$

where $\theta(x, t)$ is the absolute temperature field and $\eta(x, t)$ mass specific entropy.

- **Constitutive relations (CRs):** Consider the Helmholtz energy functional Ψ

Principle of material objectivity enables

$$\Psi = \hat{\Psi}(\nabla_s \mathbf{u}, \theta, \nabla\theta, \mathbf{M}^R, \mathbf{M}^E) \rightarrow \dot{\Psi} = \partial_{\boldsymbol{\varepsilon}} \hat{\Psi} \dot{\boldsymbol{\varepsilon}} + \partial_{\theta} \hat{\Psi} \dot{\theta} + \partial_{\nabla\theta} \hat{\Psi} \dot{\nabla\theta} + \partial_{\mathbf{M}^R} \hat{\Psi} \dot{\mathbf{M}^R}^0 + \partial_{\mathbf{M}^E} \hat{\Psi} \dot{\mathbf{M}^E}^0$$

Insertion of $\dot{\Psi}$ to CPI yields:

$$[\boldsymbol{\sigma} - \rho\partial_{\boldsymbol{\varepsilon}} \hat{\Psi}] \dot{\boldsymbol{\varepsilon}} - \rho [\eta + \partial_{\theta} \hat{\Psi}] \dot{\theta} - [\partial_{\nabla\theta} \hat{\Psi}] \dot{\nabla\theta} - \frac{1}{\theta} \mathbf{q} \cdot \nabla\theta \geq 0$$

$$\text{CRs: } [\boldsymbol{\sigma} - \rho\partial_{\boldsymbol{\varepsilon}} \hat{\Psi}] = 0; \quad [\eta + \partial_{\theta} \hat{\Psi}] = 0; \quad [\rho\partial_{\nabla\theta} \hat{\Psi}] = 0; \quad \text{Fourier relation: } \mathbf{q} = -\kappa \nabla\theta$$

\therefore **Thermodynamic consistency** is satisfied; **Closure problem** is fulfilled.

Closure	
#eqns	#unkns
1 _(mass)	+1(ρ)
3 _(Imom.)	+3(\mathbf{v})
1 _(energy)	+9($\boldsymbol{\sigma}$)
	+0(\mathbf{b})
	+0(r)
	+3(\mathbf{q})
	-3($\boldsymbol{\sigma}$)
	+1(η)
	+1(θ)
	+6($\boldsymbol{\sigma}$)
	+1(η)
	+3(\mathbf{q})
15	15

2. Mathematical modeling for thermodynamic-consistent solid-state electrolyte

- Helmholtz energy functional

$$\Psi = \hat{\Psi}(\nabla_s \mathbf{u}, \theta, \cancel{\nabla \theta}, \mathbf{M}) = \hat{\Psi}(\boldsymbol{\varepsilon}, \theta, \mathbf{M}) = \tilde{\Psi}_{\text{elastic}}(\boldsymbol{\varepsilon}, \mathbf{M}) + \tilde{\Psi}_{\text{thermal}}(\theta) + \tilde{\Psi}_{\text{thermo-elastic}}(\boldsymbol{\varepsilon}, \mathbf{M}, \theta)$$

Isothermal: $\Psi = \tilde{\Psi}_{\text{elastic}}(\boldsymbol{\varepsilon}, \mathbf{M}) = \tilde{\Psi}(I_1, I_2, I_3, I_4, I_5; \lambda, \mu, \alpha, \beta)$
 $= \tilde{\Psi}_{\text{isotropic}}(I_1, I_2, I_3; \lambda, \mu) + \tilde{\Psi}_{\text{anisotropic}}(I_4, I_5; \alpha) + \tilde{\Psi}_{\text{coupling}}(I_1, I_2, I_3, I_4, I_5; \beta)$

where

$$I_1 = \text{tr}[\boldsymbol{\varepsilon}], \quad I_2 = \text{tr}[\boldsymbol{\varepsilon}^2], \quad I_3 = \text{tr}[\boldsymbol{\varepsilon}^3], \quad I_4 = \text{tr}[\boldsymbol{\varepsilon} \mathbf{M}], \quad I_5 = \text{tr}[\boldsymbol{\varepsilon}^2 \mathbf{M}]$$

- Constitutive relations

Stress tensor

$$\boldsymbol{\sigma} = \partial_{\boldsymbol{\varepsilon}} \tilde{\Psi} = \partial_{\boldsymbol{\varepsilon}} \tilde{\Psi}_{\text{isotropic}} + \partial_{\boldsymbol{\varepsilon}} \tilde{\Psi}_{\text{anisotropic}} + \partial_{\boldsymbol{\varepsilon}} \tilde{\Psi}_{\text{coupling}}$$

Tangent modulus

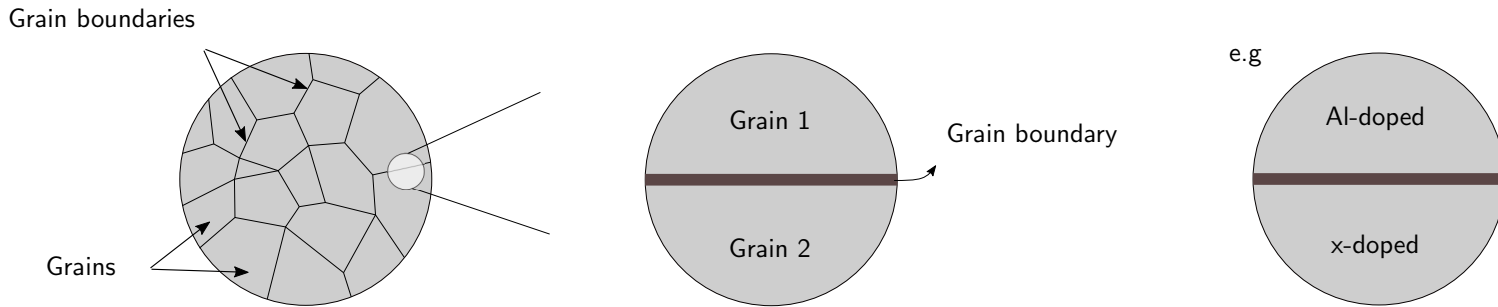
$$\mathbb{C} = \partial_{\boldsymbol{\varepsilon} \boldsymbol{\varepsilon}} \tilde{\Psi} = \partial_{\boldsymbol{\varepsilon}} \boldsymbol{\sigma} = \partial_{\boldsymbol{\varepsilon} \boldsymbol{\varepsilon}} \tilde{\Psi}_{\text{isotropic}} + \partial_{\boldsymbol{\varepsilon} \boldsymbol{\varepsilon}} \tilde{\Psi}_{\text{anisotropic}} + \partial_{\boldsymbol{\varepsilon} \boldsymbol{\varepsilon}} \tilde{\Psi}_{\text{coupling}}$$

Hookean relation:

$$\therefore \boxed{\boldsymbol{\sigma} = \mathbb{C} \boldsymbol{\varepsilon}}$$

3. Numerical implementation, representative results and applications

Overview of problem to solve

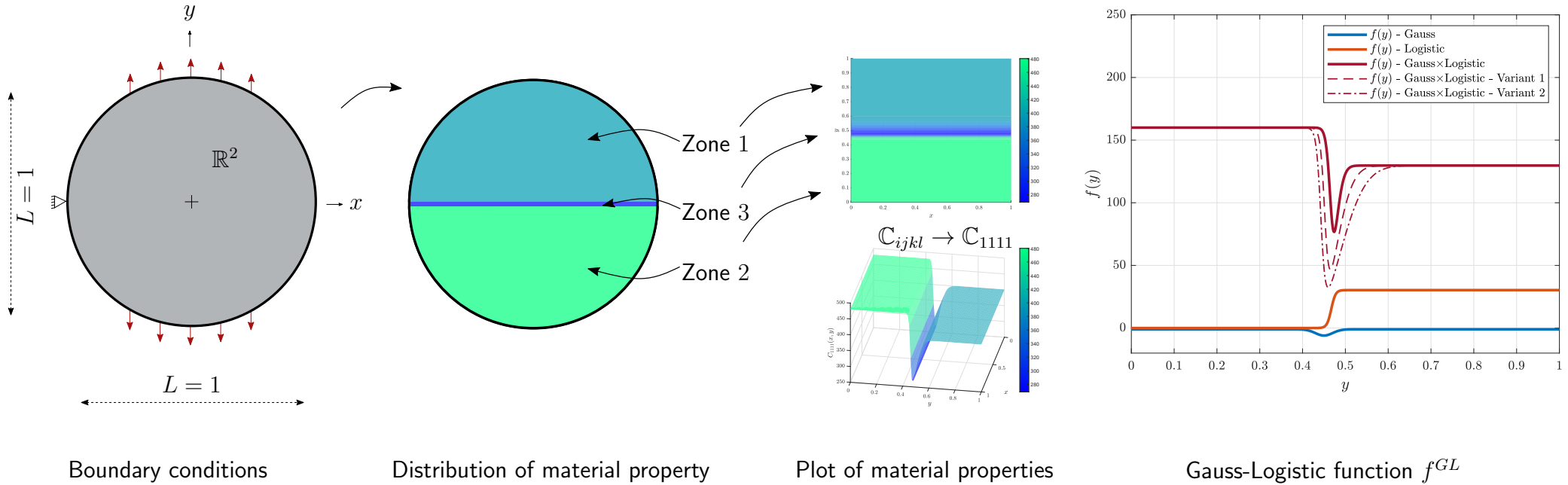


To discuss in the next slides:

- Grain 1 behaves **differently** from Grain 2: **material properties + misorientations**
- **Mobility function** f^{GL} for material properties
- **Spatial dependence** of tangent modulus C_{ijkl}
- Connection of grain boundary and **Griffith criterion** x_{Griff}
- Relationship of **strain energy** (Continuum) and **surface energy** (DFT) with Griffith criterion

3. Numerical implementation, representative results and applications

Setting up model: Definition of boundary conditions and Gauss-Logistic function f^{GL}

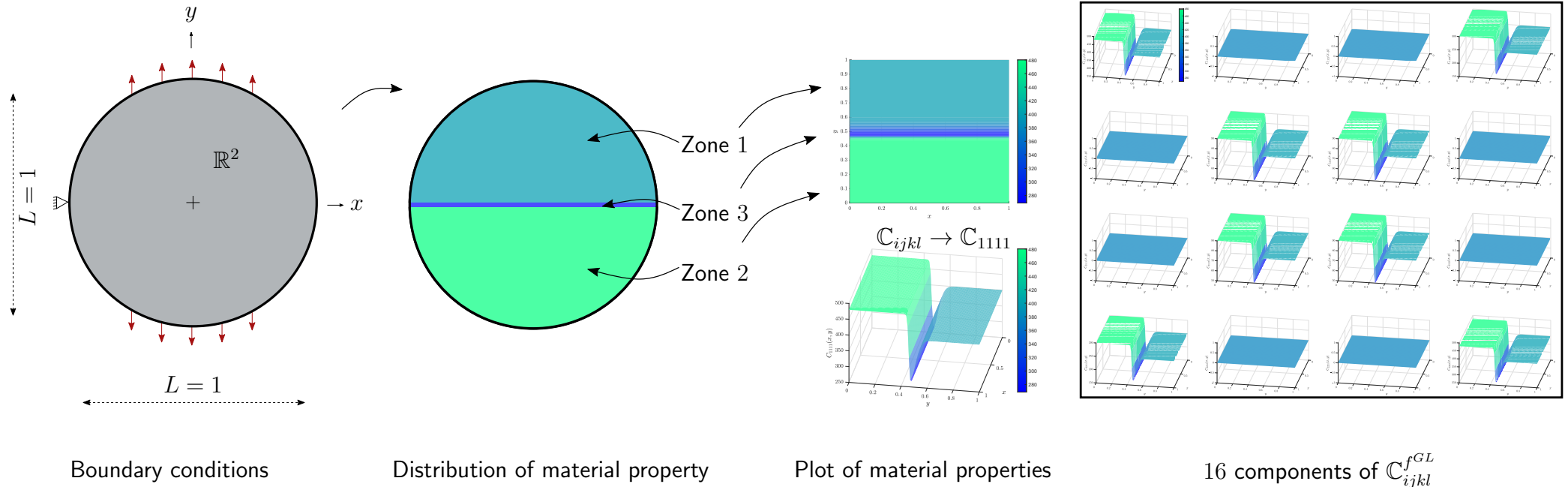


- Dirichlet BC $\partial\Omega_u$ is fixed at $\mathbf{u}_{\text{left-most}} = \mathbf{0}$; Neumann BC are applied on $\mathbf{t}_{\text{upper-parts}} = \bar{\mathbf{t}}_{\text{upper}}$ and $\mathbf{t}_{\text{lower-parts}} = \bar{\mathbf{t}}_{\text{lower}}$.
- Physical domain Ω includes 3 zones: Zone 1 and 2 aimed for *grains*; Zone 3 for *grain boundary*.
- The two Lamé functions $f_\lambda^{GL}(y)$ and $f_\mu^{GL}(y)$ depend on space and govern material properties of the bulk.
- Gauss-Logistic function $f^{GL}(y; \nu_1, \nu_2, \nu_3, \nu_4, \nu_5, \nu_6)$ defines the two Lamé constants across grain boundary:

$$f^{GL}(y) = - \underbrace{\left(\nu_1 \exp \left(-\frac{(y - \nu_2)^2}{2 \times \nu_5^2} \right) + 1 \right)}_{=f^G(y)} \times \underbrace{\left(\frac{1}{\nu_6 + \exp(-\nu_3 \times (y - \nu_2))} \right)}_{=f^L(y)} + \nu_4$$

3. Numerical implementation, representative results and applications

Setting up model: Definition of boundary conditions and Gauss-Logistic function f^{GL}



- Dirichlet BC $\partial\Omega_u$ is fixed at $\mathbf{u}_{\text{left-most}} = \mathbf{0}$; Neumann BC are applied on $\mathbf{t}_{\text{upper-parts}} = \bar{\mathbf{t}}_{\text{upper}}$ and $\mathbf{t}_{\text{lower-parts}} = \bar{\mathbf{t}}_{\text{lower}}$.
- Physical domain Ω includes 3 zones: Zone 1 and 2 aimed for *grains*; Zone 3 for *grain boundary*.
- The two Lamé functions $f_\lambda^{GL}(y)$ and $f_\mu^{GL}(y)$ depend on space and govern material properties of the bulk.
- Gauss-Logistic function $f^{GL}(y; \nu_1, \nu_2, \nu_3, \nu_4, \nu_5, \nu_6)$ defines the two Lamé constants across grain boundary:

$$f^{GL}(y) = - \underbrace{\left(\nu_1 \exp \left(-\frac{(y - \nu_2)^2}{2 \times \nu_5^2} \right) + 1 \right)}_{=f^G(y)} \times \underbrace{\left(\frac{1}{\nu_6 + \exp(-\nu_3 \times (y - \nu_2))} \right)}_{=f^L(y)} + \nu_4$$

3. Numerical implementation, representative results and applications

Problem to solve: From the conservation law of linear momentum: Find displacement u_i such that

- **Strong form:** Governing PDE for vector-unknown displacement u with sufficient boundary conditions given

$$\nabla \cdot \mathbb{C}^{f^{GL}}(y) \nabla_s u + \rho b = 0$$

which is a system of interlocking unknowns u_i and written in index notation as follows

PDE	$\sigma_{ij,j} + \rho b_i = 0$
Constitutive relation	$\sigma_{ij} = \mathbb{C}_{ijkl}^{f^{GL}}(y) \varepsilon_{kl}$
Kinematic relation	$\varepsilon_{kl} = \frac{1}{2} \left(\frac{\partial u_k}{\partial x_l} + \frac{\partial u_l}{\partial x_k} \right)$
Dirichlet BC	$u_i = \bar{u}_i$ on $\partial\Omega_{u_i}$
Neumann BC	$\sigma_{ij} n_j = \bar{t}_i$ on $\partial\Omega_{t_i}$

where $\mathbb{C}_{ijkl}^{f^{GL}}(y) \triangleq \hat{\mathbb{C}}(\mathbf{f}_\lambda^{GL}(y), \mathbf{f}_\mu^{GL}(y))$

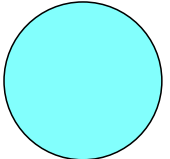
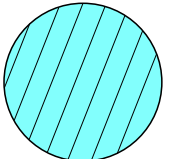
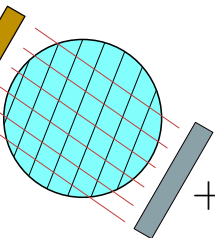
- **Weak form:** Seeking solutions numerically

$$\sum_e^{\#_e} \int_{\Omega^e} \delta u_{i,j}^e \mathbb{C}_{ijkl}^{f^{GL}}(y) u_{k,l}^e d\Omega^e = \sum_e^{\#_e} \int_{\Omega^e} \delta u_i^e \rho b_i d\Omega^e + \sum_e^{\#_e} \int_{\partial\Omega_{t_i}^e} \delta u_i^e \bar{t}_i d\partial\Omega^e$$

→ The tangent modulus $\mathbb{C}_{ijkl}^{f^{GL}}(y)$ is a 4th order tensor and its entries are **spatially dependent** in y-direction.

3. Numerical implementation, representative results and applications

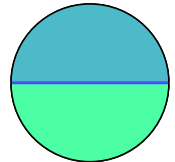
Applications: Variants of \mathbb{C}_{ijkl} and their use-cases

1st		$\mathbb{C}_{ijkl} \triangleq \lambda \mathbf{1} \otimes \mathbf{1} + 2\mu \mathbb{I}$
2nd		$\begin{aligned} \mathbb{C}_{ijkl}^{\mathbf{d}^R} &\triangleq \lambda \mathbf{1} \otimes \mathbf{1} + 2\mu \mathbb{I} \\ &+ \alpha^R (\mathbf{M}^R \otimes \mathbf{1} + \mathbf{1} \otimes \mathbf{M}^R) + 2\mu \mathbb{I}_{\mathbf{d}^R} + \beta^R \mathbf{M}^R \otimes \mathbf{M}^R \end{aligned}$
3rd		$\begin{aligned} \mathbb{C}_{ijkl}^{\mathbf{d}^R \circ \mathbf{d}^E} &\triangleq \lambda \mathbf{1} \otimes \mathbf{1} + 2\mu \mathbb{I} \\ &+ \alpha^R (\mathbf{M}^R \otimes \mathbf{1} + \mathbf{1} \otimes \mathbf{M}^R) + 2\mu \mathbb{I}_{\mathbf{d}^R} + \beta^R \mathbf{M}^R \otimes \mathbf{M}^R \\ &+ \alpha^E (\mathbf{M}^E \otimes \mathbf{1} + \mathbf{1} \otimes \mathbf{M}^E) + \delta^E \mathbb{I}_{\mathbf{d}_E} + \beta^E \mathbf{M}^E \otimes \mathbf{M}^E \\ &+ \gamma (\mathbf{M}^E \otimes \mathbf{M}^R + \mathbf{M}^R \otimes \mathbf{M}^E) \end{aligned}$

3. Numerical implementation, representative results and applications

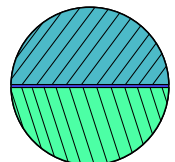
Applications: Variants of \mathbb{C}_{ijkl} and their use-cases

4th



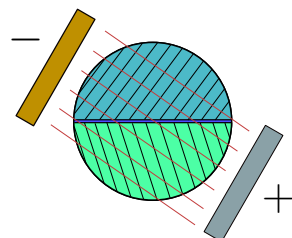
$$\mathbb{C}_{ijkl}^{f^{GL}}(y) \triangleq f_{\lambda}^{GL}(y) \mathbf{1} \otimes \mathbf{1} + 2f_{\mu}^{GL}(y) \mathbb{I}$$

5th



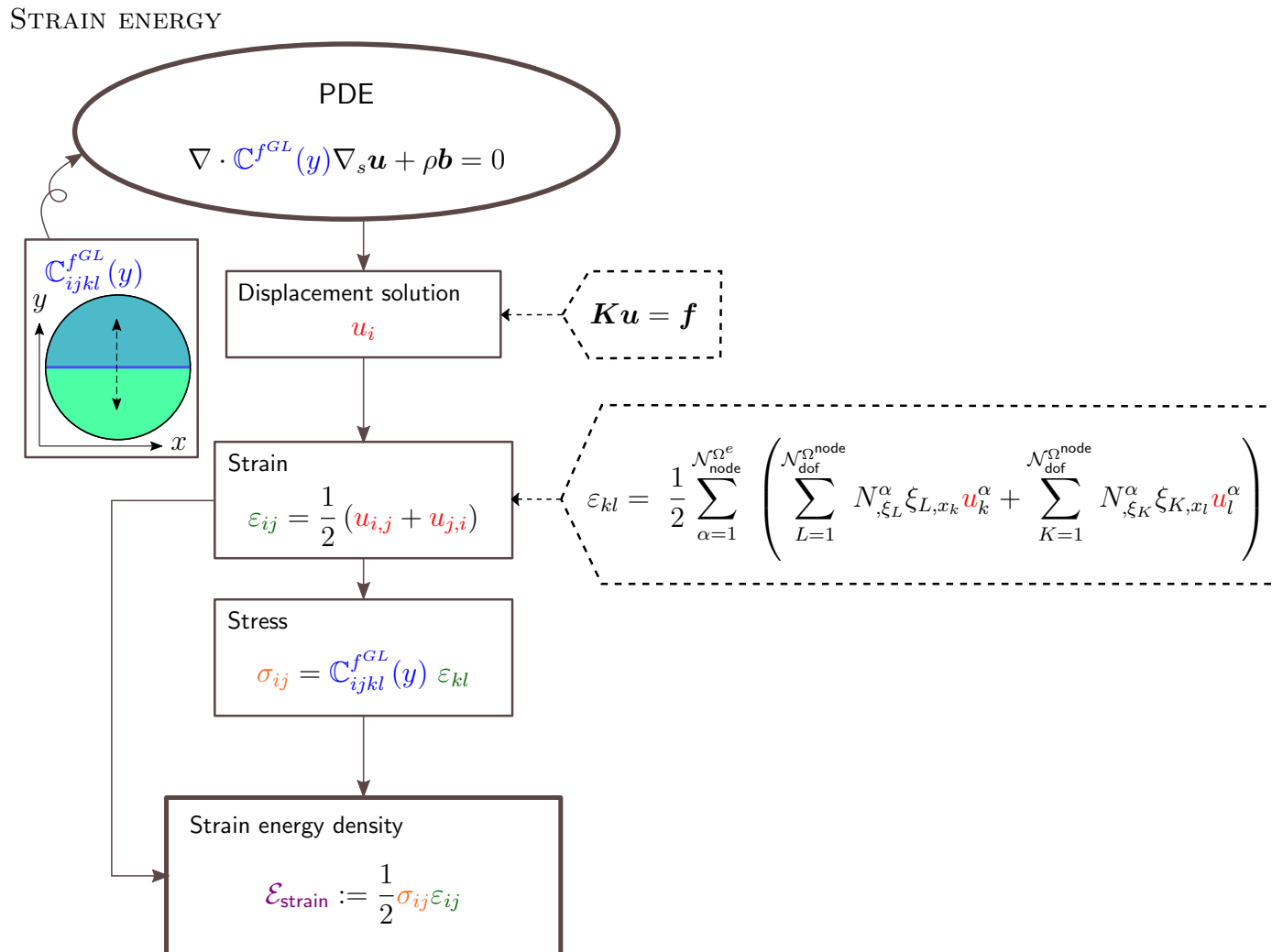
$$\begin{aligned} \mathbb{C}_{ijkl}^{f_{d^R}^{GL}}(y) &\triangleq f_{\lambda}^{GL}(y) \mathbf{1} \otimes \mathbf{1} + 2f_{\mu}^{GL}(y) \mathbb{I} \\ &+ f_{\alpha^R}^{GL}(y) \left(\mathbf{M}^{f_R^{GL}} \otimes \mathbf{1} + \mathbf{1} \otimes \mathbf{M}^{f_R^{GL}} \right) + 2f_{\mu}^{GL}(y) \mathbb{I}_{d^{f_R^{GL}}} + f_{\beta^R}^{GL}(y) \mathbf{M}^{f_R^{GL}} \otimes \mathbf{M}^{f_R^{GL}} \end{aligned}$$

6th



$$\begin{aligned} \mathbb{C}_{ijkl}^{f_{d^R \circ d^E}^{GL}}(y) &\triangleq f_{\lambda}^{GL}(y) \mathbf{1} \otimes \mathbf{1} + 2f_{\mu}^{GL}(y) \mathbb{I} \\ &+ f_{\alpha^R}^{GL}(y) \left(\mathbf{M}^{f_R^{GL}} \otimes \mathbf{1} + \mathbf{1} \otimes \mathbf{M}^{f_R^{GL}} \right) + 2f_{\mu}^{GL}(y) \mathbb{I}_{d^{f_R^{GL}}} + f_{\beta^R}^{GL}(y) \mathbf{M}^{f_R^{GL}} \otimes \mathbf{M}^{f_R^{GL}} \\ &+ \alpha^E \left(\mathbf{M}^E \otimes \mathbf{1} + \mathbf{1} \otimes \mathbf{M}^E \right) + \delta^E \mathbb{I}_{d_E} + \beta^E \mathbf{M}^E \otimes \mathbf{M}^E \\ &+ f_{\gamma}^{GL}(y) \left(\mathbf{M}^E \otimes \mathbf{M}^{f_R^{GL}} + \mathbf{M}^{f_R^{GL}} \otimes \mathbf{M}^E \right) \end{aligned}$$

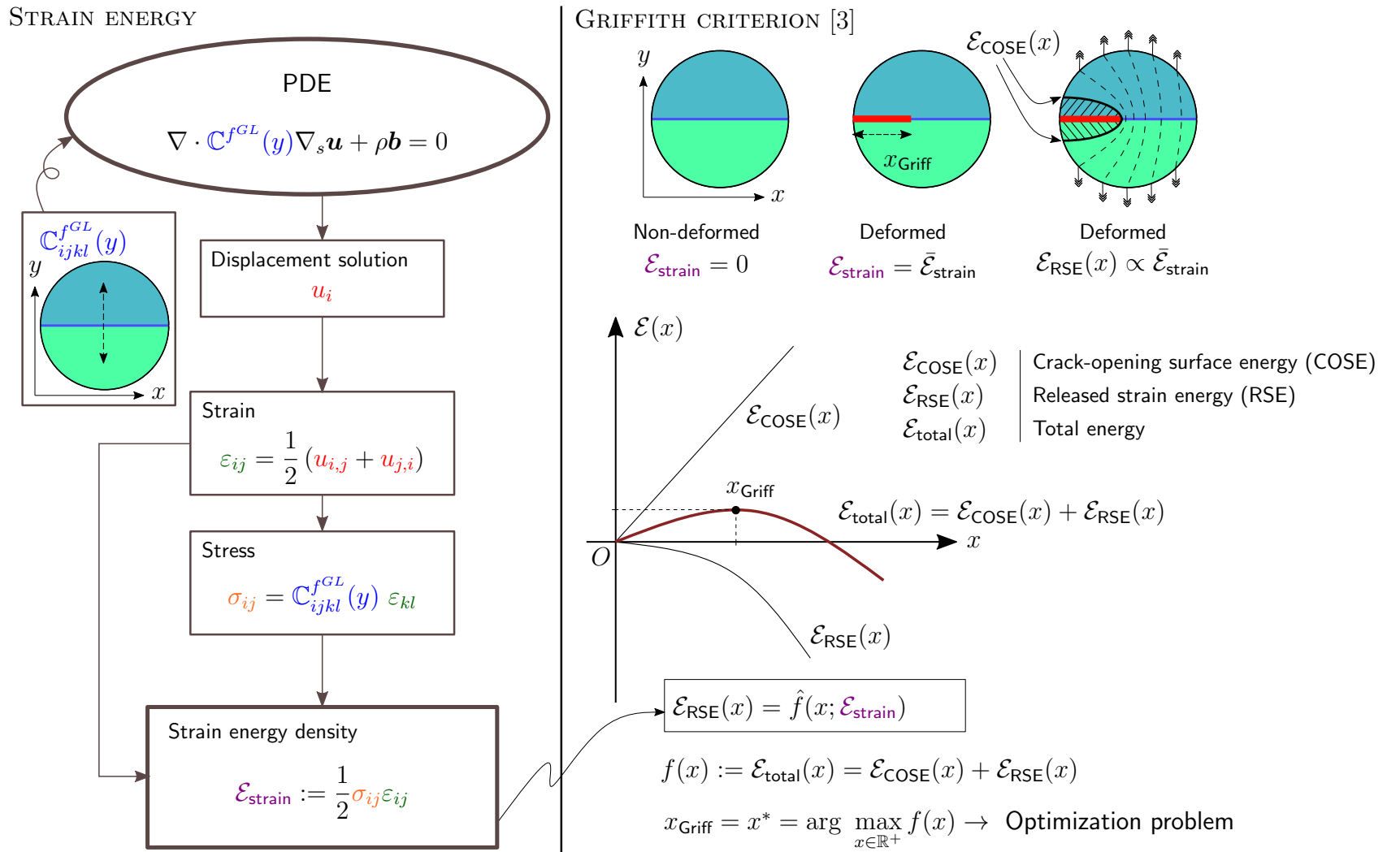
3. Application: Griffith criterion x_{Griff} and Strain energy $\mathcal{E}_{\text{strain}}$



→ Strain energy $\mathcal{E}_{\text{strain}}$ offers essential information for Griffith criterion x_{Griff} analysis.

→ Griffith criterion x_{Griff} is the **critical virtual crack length**, which is a useful measure for solid material failure.

3. Application: Griffith criterion x_{Griff} and Strain energy $\mathcal{E}_{\text{strain}}$

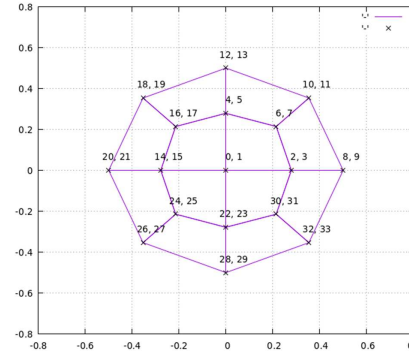
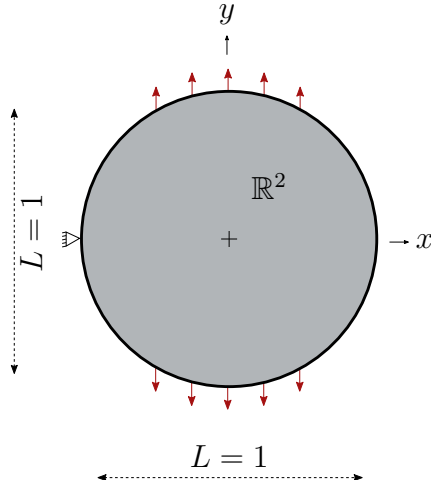


→ Strain energy $\mathcal{E}_{\text{strain}}$ offers essential information for Griffith criterion x_{Griff} analysis.

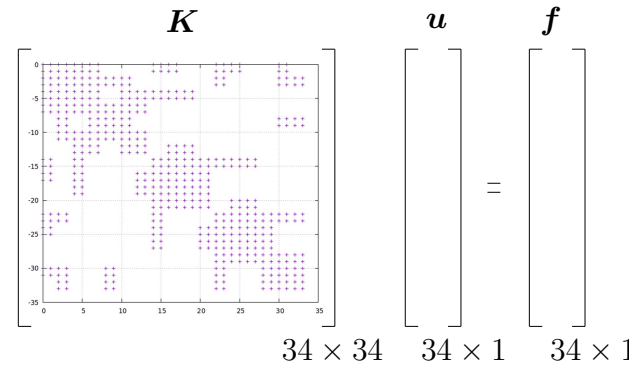
→ Griffith criterion x_{Griff} is the **critical virtual crack length**, which is a useful measure for solid material failure.

3. Numerical implementation, representative results and applications

Use-case 1: Circle domain; \mathbb{C}_{ijkl} displacement solution



12 elements; 34 dofs.



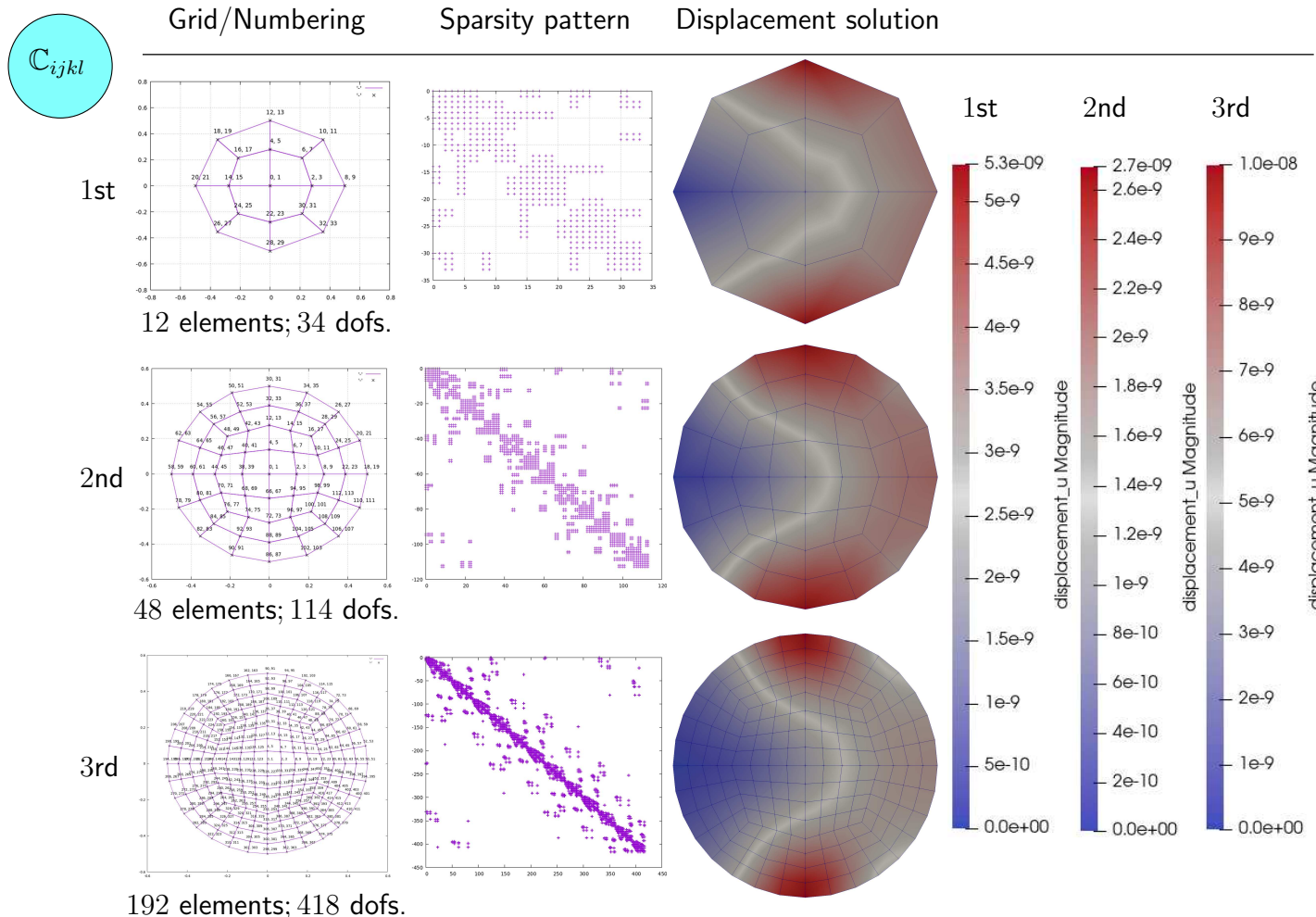
- Derivation of weak form leads to a system of linear algebraic equations: $\mathbf{K}\mathbf{u} = \mathbf{f} \rightarrow$ Solve for \mathbf{u} .
- Element stiffness matrix \mathbf{K}^e : known; approximated by Gauss quadrature rule; index notation implies 4 + 2 for-loop:

$$K_{ik}^{\alpha\beta} = \int_{\Omega^\xi} \left(\mathcal{L}_1^\alpha \mathbb{C}_{i1k1}^{fGL}(y) \mathcal{R}_1^\beta + \mathcal{L}_1^\alpha \mathbb{C}_{i1k2}^{fGL}(y) \mathcal{R}_2^\beta + \mathcal{L}_2^\alpha \mathbb{C}_{i2k1}^{fGL}(y) \mathcal{R}_1^\beta + \mathcal{L}_2^\alpha \mathbb{C}_{i2k2}^{fGL}(y) \mathcal{R}_2^\beta \right) \det(\mathbf{J}) d\Omega^\xi$$

where \mathcal{L}_j^α and \mathcal{R}_l^β are gradients of basis functions at node α^{th} and β^{th} , respectively.

3. Numerical implementation, representative results and applications

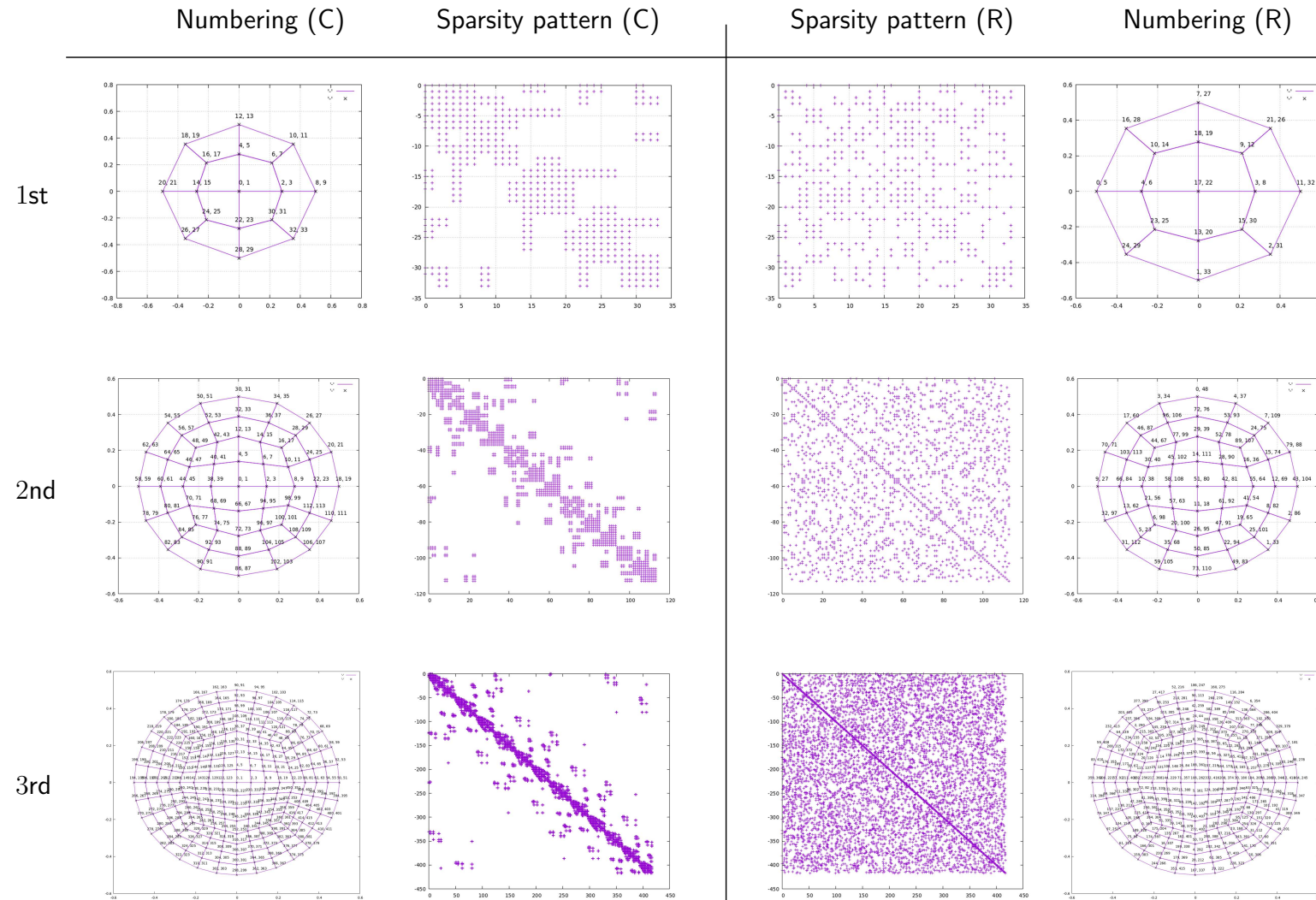
Use-case 1: Circle domain; \mathbb{C}_{ijkl} displacement solution



Observations

- Color gradient illustrates solution of displacement.
- Higher number of used elements lead to sparsity pattern for the assembled K .

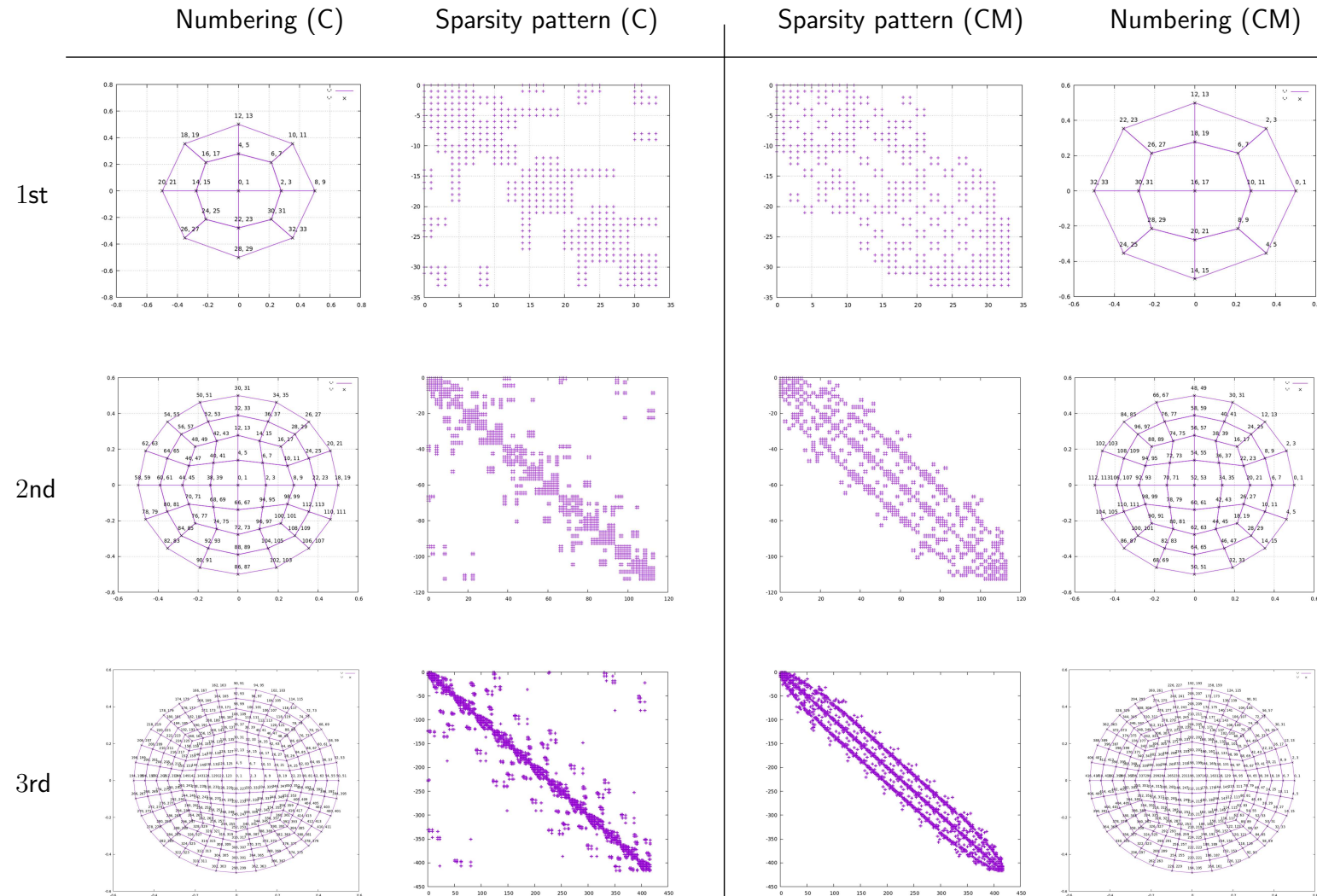
3. Conventional (C) numbering grid vs Random (R) numbering grid



Observations

- Sparsity degree of an assembled K matrix depends on the way of numbering over elements.
- Different strategy of numbering can help to reduce the degree of sparsity.

3. Conventional (C) numbering grid vs Cuthill-McKee (CM) numbering grid

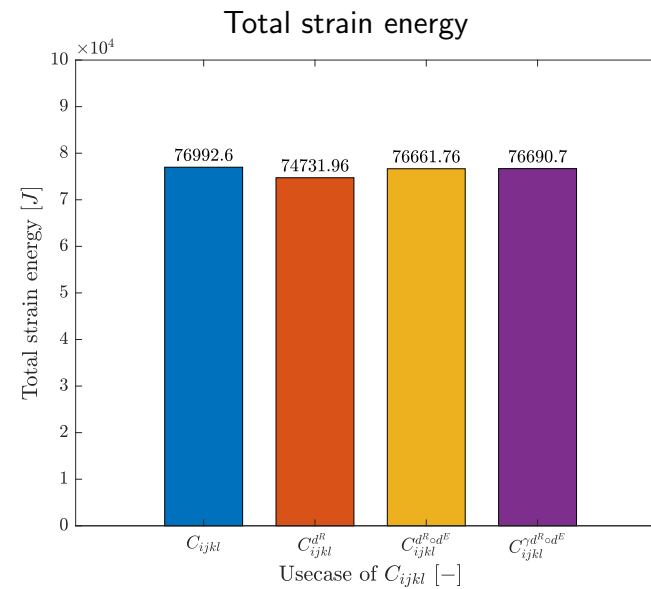
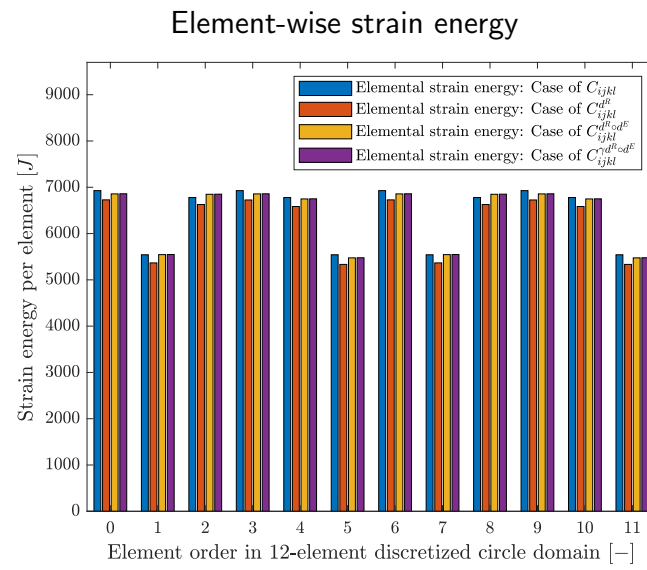
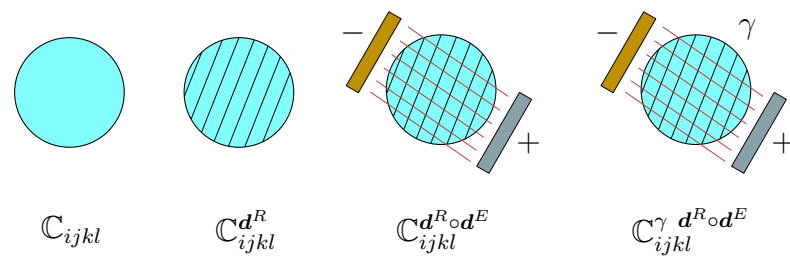
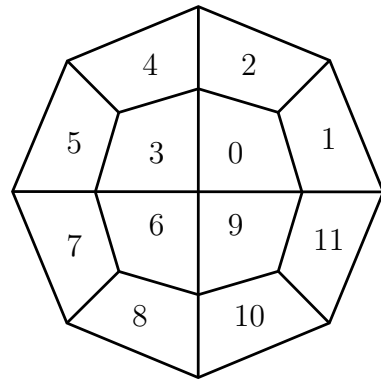


Observations

- Sparsity degree of an assembled K matrix depends on the way of numbering over elements.
- Different strategy of numbering can help to reduce the degree of sparsity.

3. Application: Griffith criterion x_{Griff} and Strain energy $\mathcal{E}_{\text{strain}}$

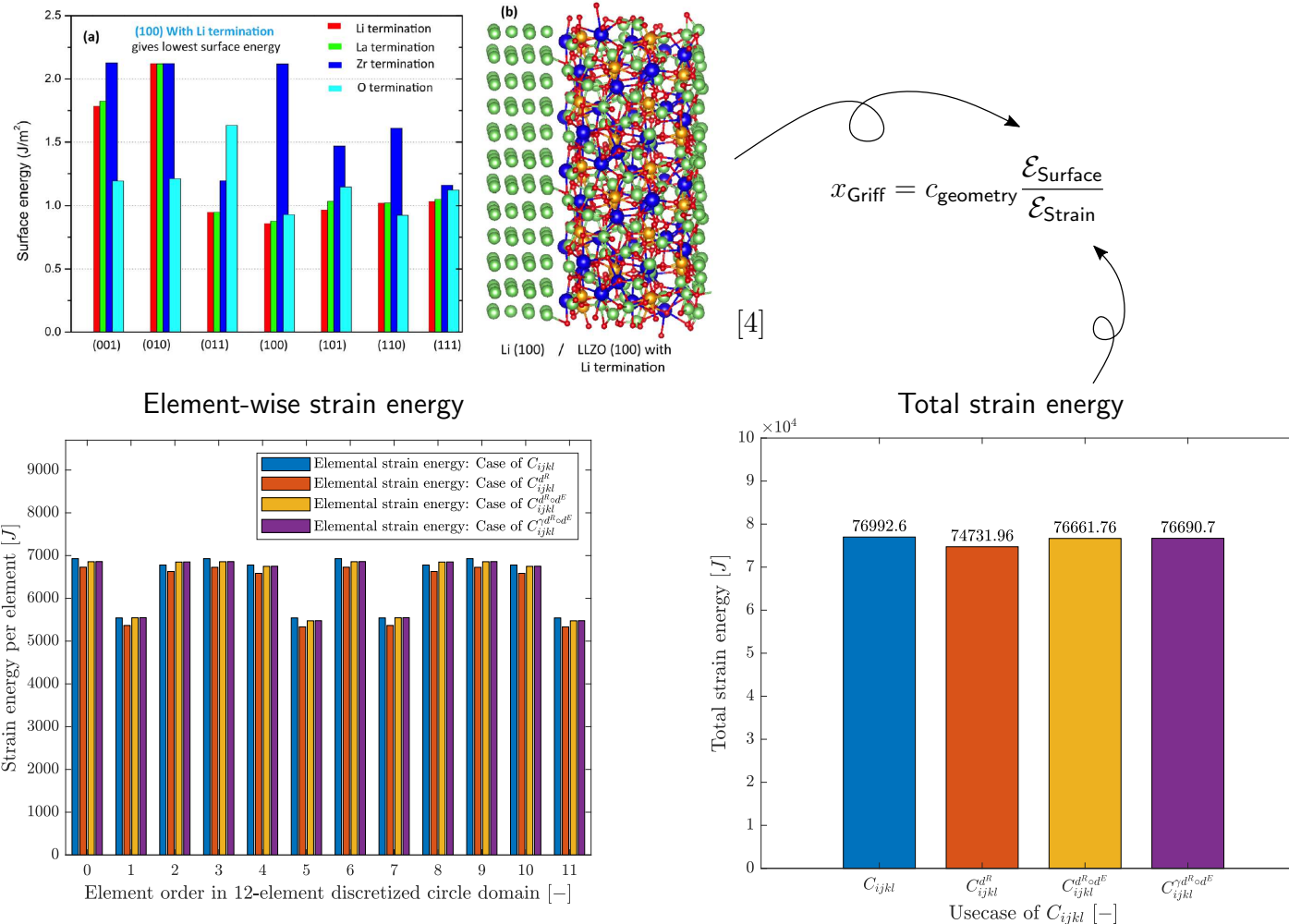
Representative strain energy results $\mathcal{E}_{\text{strain}}$



- Every element in discretized domain contributes to the total strain energy.
- Different use-cases of C_{ijkl} lead to various strain energy.

3. Application: Griffith criterion x_{Griff} and Strain energy $\mathcal{E}_{\text{strain}}$

Surface energy $\mathcal{E}_{\text{surface}}$ and Griffith criterion x_{Griff}



- In a monograph, Griffith criterion x_{Griff} is proportional to $\mathcal{E}_{\text{surface}}$ and disproportional to $\mathcal{E}_{\text{strain}}$.
- Surface energy $\mathcal{E}_{\text{surface}}$ is studied from DFT, while strain energy $\mathcal{E}_{\text{strain}}$ from continuum models.

4. Summary and conclusions

Results obtained

- Post-processing done for stress, strain and strain energy, which is essential for Griffith criterion analysis.
- Representative strain energy solution for Usecases is computed.
- Directional effect has been modeled and spatial dependence problem has been described.

Ongoing and future research directions

- (Time-dependent) implementation @ JURECA + Numerical analysis + Validations + Verification.
- Coupled electro-magneto-chemo-thermo-elastic problems could be taken into consideration.
- Scale bridging into quantum physics: Update information from quantum for continuum model.
- Dendrite formation: advection - diffusion - transport problem.

References

- [1] Controlling and correlating the effect of grain size with the mechanical and electrochemical properties of $\text{Li}_7\text{La}_3\text{Zr}_2\text{O}_{12}$ solid-state electrolyte, Sharafi et al. [2017]
- [2] The Role of Local Inhomogeneities on Dendrite Growth in LLZO-Based Solid Electrolytes, Barai et al. [2020]
- [3] The phenomena of rupture and flow in solids, Griffith [1921]
- [4] Nanoscale Imaging of Fundamental Li Battery Chemistry: Solid-Electrolyte Interphase Formation and Preferential Growth of Lithium Metal Nanoclusters, Sacci et al. [2015]

Backup

Test cases: Square domain: 1 element

Order of basis functions	$\mathcal{N}_{\text{DOFs}}$	$\left(K_{ik}^{\alpha\beta} \right)_{\text{size}}$	$\mathcal{N}_{\text{integrals}}$	$(\mathcal{N}_{\text{integrals}})^{\text{Matlab time}}$	Plot of basis functions
Linear	8	$K_{8 \times 8}$	64	~ 20 mins	
Quadratic	18	$K_{18 \times 18}$	324	~ 40 mins	
Cubic	32	$K_{32 \times 32}$	1024	~ 3 hours	
Quartic	50	$K_{50 \times 50}$	2500	~ 6 hours	

Boundary conditions

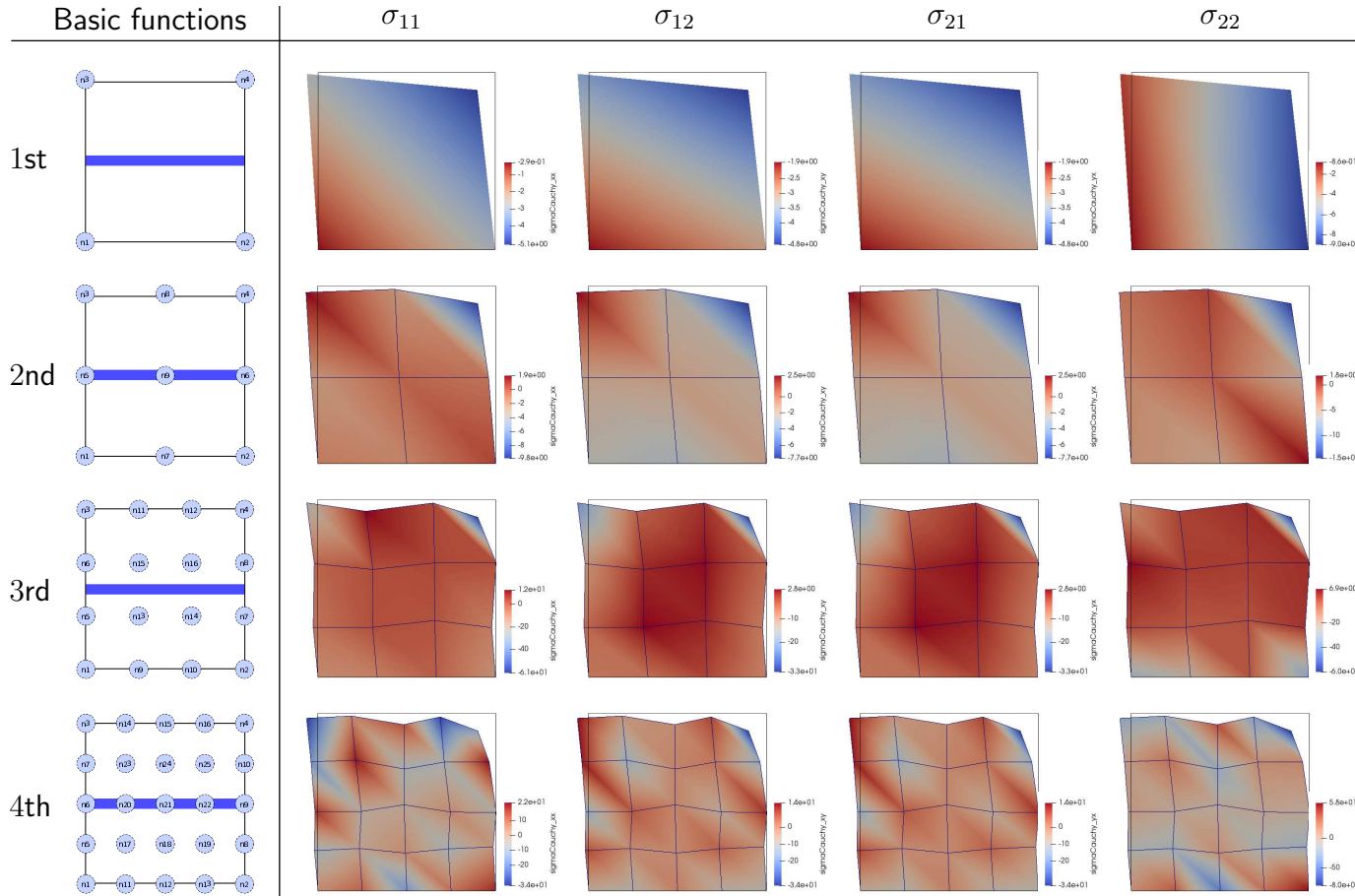
- Derivation of weak form leads to a system of linear algebraic equations: $\mathbf{K}^e \mathbf{u}^e = \mathbf{f}^e \rightarrow \text{Solve for } \mathbf{u}^e.$
- Element stiffness matrix \mathbf{K}^e : known; approximated by Gauss quadrature rule; index notation implies 4 + 2 for-loop:

$$K_{ik}^{\alpha\beta} = \int_{\Omega^\xi} \left(\mathcal{L}_1^\alpha \mathbb{C}_{i1k1}^{fGL}(y) \mathcal{R}_1^\beta + \mathcal{L}_1^\alpha \mathbb{C}_{i1k2}^{fGL}(y) \mathcal{R}_2^\beta + \mathcal{L}_2^\alpha \mathbb{C}_{i2k1}^{fGL}(y) \mathcal{R}_1^\beta + \mathcal{L}_2^\alpha \mathbb{C}_{i2k2}^{fGL}(y) \mathcal{R}_2^\beta \right) \det(\mathbf{J}) d\Omega^\xi$$

where \mathcal{L}_j^α and \mathcal{R}_l^β are gradients of basis functions at node α^{th} and β^{th} , respectively.

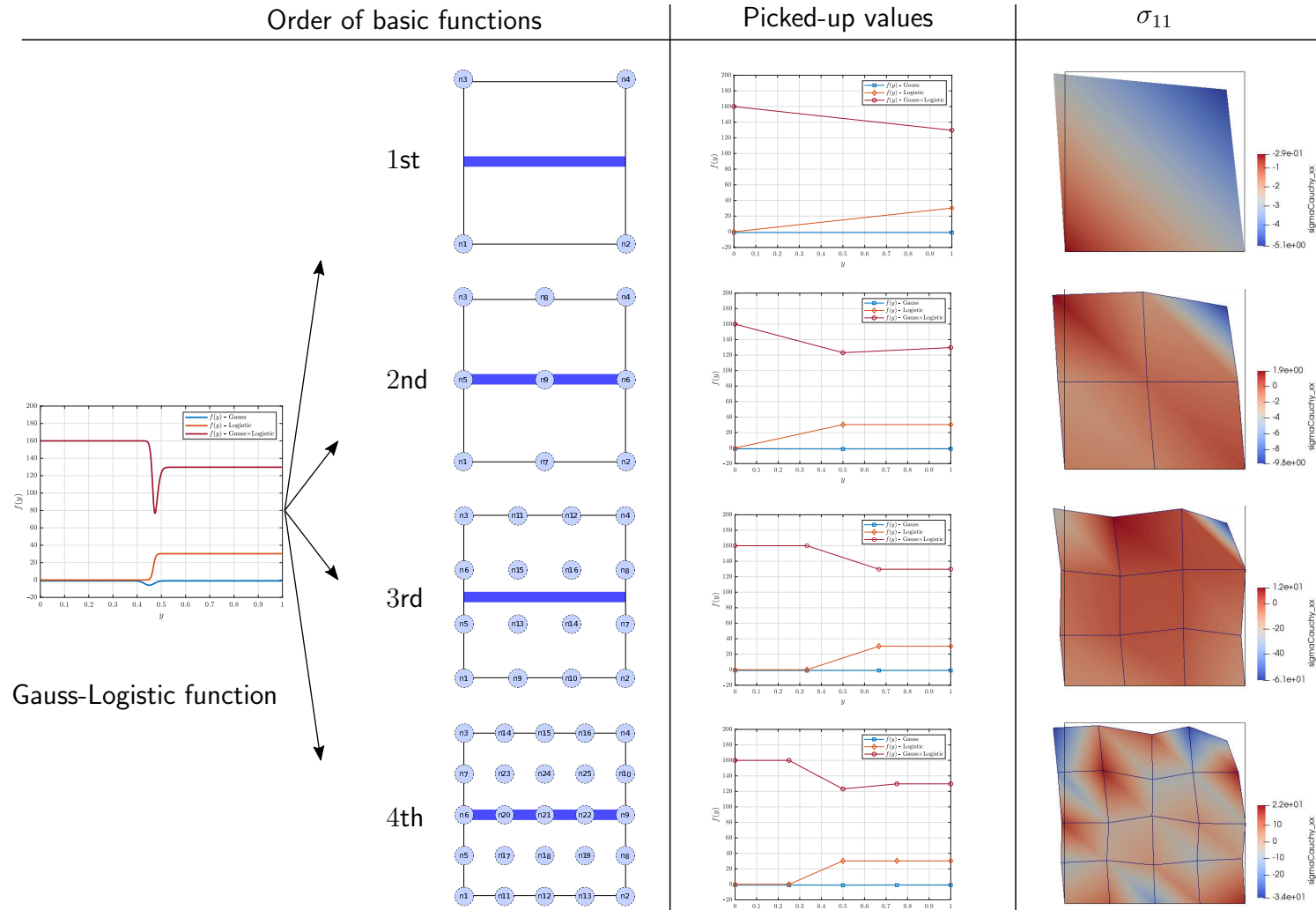
Backup

Stress solution: $\sigma_{ij} = \mathbb{C}_{ijkl}^{fGL}(y) \quad \varepsilon_{kl} = \mathbb{C}_{ijkl}^{fGL}(y) \quad \frac{1}{2} \sum_{\alpha=1}^{\mathcal{N}_{\text{node}}^{\Omega^e}} \left(\sum_{L=1}^{\mathcal{N}_{\text{dof}}^{\text{node}}} N_{,\xi_L}^\alpha \xi_{L,x_k} u_k^\alpha + \sum_{K=1}^{\mathcal{N}_{\text{dof}}^{\text{node}}} N_{,\xi_K}^\alpha \xi_{K,x_l} u_l^\alpha \right)$



- Observations**
- Stress solution σ_{ij} is of interest as it links to Gauss-Logistic-based tangent modulus $\mathbb{C}_{ijkl}^{fGL}(y)$.
 - Color gradient illustrates solution of stress distributed over physical domain Ω .

Backup: Stress solution explanation



- Possibilities**
- Increase the order of basis functions.
 - Distribute more nodes at and surrounding *areas of much-more-deformation*.